Hydrobiologia **247**: 141–161, 1992.
V. Jaccarini & E. Martens (eds), The Ecology of Mangrove and Related Ecosystems.

Hydrodynamics of mangrove swamps and their coastal waters

Eric Wolanski
Australian Institute of Marine Science, P.M.B. No. 3, Townsville M.C., Qld. 4810, Australia

Abstract

Mangrove swamps help control the tidal hydrodynamics of many tropical estuaries. They generate an asymmetry of the tidal currents in both the tidal creeks and the mangrove swamps. This results in self-scouring of the tidal channels. Mangrove land reclamation results in siltation of the channel. Mangrove swamps control the flushing rates of the estuaries through the lateral trapping effect. Lateral trapping leads to the aggregation of mangrove litter along slick lines. Evapotranspiration plays a role in the hot dry season by forming a salinity maximum zone which isolates the estuary from the coastal waters for several months of the year. In the absence of runoff, evapotranspiration in the hot dry season generates an inverse estuarine circulation which can trap high salinity mangrove water, and mangrove detritus, along the bottom of a mangrove creek. This bottom layer can become anaerobic. Groundwater flow appears to play a key role in the nutrient budget of mangrove creeks, exporting salt left behind by evapotranspiration, and inhibiting runoff after rainfall. Particulates and dissolved nutrients outwelled from mangrove swamps to coastal waters are retained in a coastal boundary layer. This coastal boundary layer water can be trapped along the shore for long periods if the coast is straight and mangrove-fringed and the coastal waters are shallow. Headlands inhibit coastal trapping because they enhance mixing. Nutrient-rich coastal boundary layer waters may be ejected offshore as tidal jets peeling off headlands and locally enriching offshore waters.

Introduction

A typical mangrove swamp is Coral Creek (Fig. 1). It is 5 km long, with fairly steep banks, and maximum depth decreasing with distance from the coast. The cross-sections can be represented by polygons (Fig. 1b). The fringing mangroves are typically 100 to 300 m wide on either side of the creek. The surface of the substrate slopes gently upwards from the creek, with elevation near the creek of about 0.3 m above mean sea level, and maximum elevation rarely exceeding 1.3 m.

When many mangrove creeks exist one next to the other, they form a large mangrove swamp. Hinchinbrook Channel (Fig. 2) is an example of such a vast mangrove swamp. The channel is 44 km long channel with 109 km^2 of open water surrounded by 164 km^2 of fringing mangrove swamps. Since the mangrove creeks draining the swamp are oriented perpendicular to the Channel, the swamp is up to 5 km wide from the dry land to the edge of the Channel.

Tidal circulation in a creek-mangrove swamp system

The barotropic tidal circulation in the Coral Creek tidal creek-mangrove system was first modeled by Wolanski *et al.* (1980). They noticed that peak tidal velocities often exceed 1 m s^{-1} in the tidal creek but never exceeded 0.07 m s^{-1} in the heavily vegetated mangrove swamps 50 m from

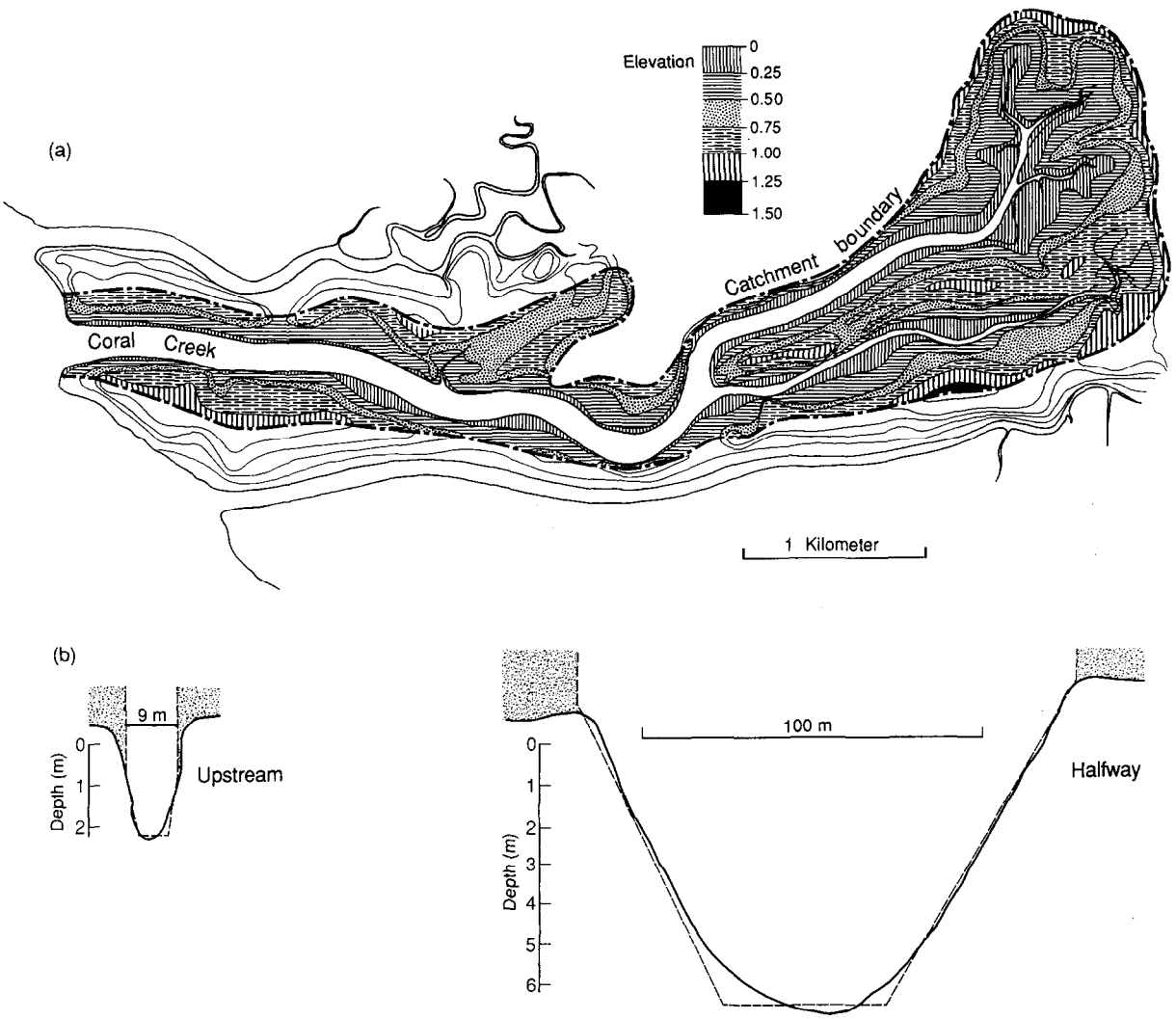

Fig. 1. (*a*) Map of Coral Creek, a mangrove creek in tropical Australia, with elevation in m. (*b*) shows two typical cross-sections in the tidal creek.

the creek. They thus divided the system in its two basic component, firstly the tidal creek where acceleration and inertia effects are important, and secondly the mangrove swamp where they are not. For modeling purposes, the swamp was divided in a number of cells of irregular shape and size fitted to the topography of the substrate (Fig. 3a). The water circulation in the swamp was calculated from the continuity equation, one such equation for each cell i,

$$\frac{\partial V_i}{\partial t} = \Sigma Q_{ij} - q_i \qquad (1)$$

where V_i is the volume of water in cell i, Q_{ij} is the discharge (in $m^3\ s^{-1}$) between cells i and j, and q_i is the discharge from cell i direct to the tidal creek. $q_i = 0$ if cell i does not touch the tidal creek. Inertia and acceleration effects are assumed to be negligible in the mangrove swamp where the momentum equation reduces to a simple balance between the frictional slope and the free surface slope,

$$S_f = \frac{\partial \eta}{\partial x} \qquad (2)$$

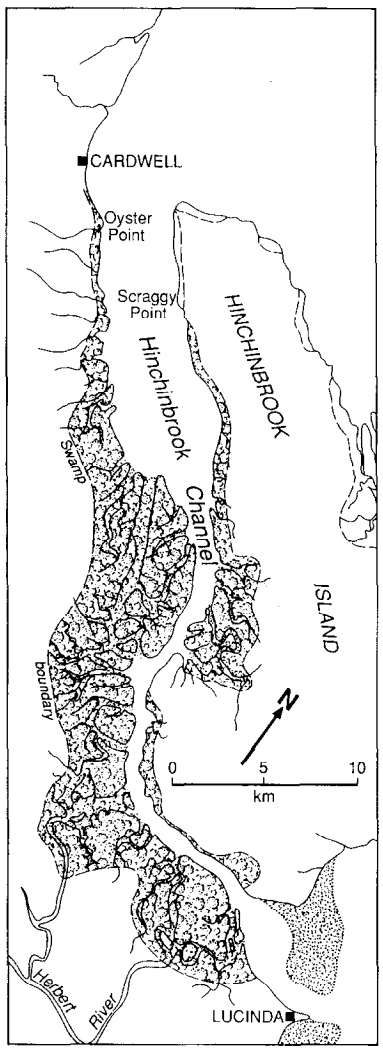

Fig. 2. Map of Hinchinbrook Channel and its fringing giant mangrove swamp, also in tropical Australia.

where η is the elevation of the water surface, x the distance and S_f the frictional slope. S_f was computed by Manning's formula and the Manning coefficient was set equal to 0.2 as characteristic of flow through dense vegetation (Petryk & Bosmajan, 1975; Wolanski *et al.*, 1980; Burke & Stolzenbach, 1983).

The tidal creek was divided in a number of cross-sections shown in Fig. 3b. In the tidal creek, acceleration and inertia effects are important and the one-dimensional barotropic equations of motion for unsteady open channel flow are

continuity:

$$\frac{\partial Q}{\partial x} + \frac{\partial A}{\partial t} = q_i \tag{3}$$

momentum:

$$\frac{\partial Q}{\partial t} + \frac{\partial}{\partial x}(Q^2/A) + gA\frac{\partial \eta}{\partial x} + gAS_f + \Delta = 0 \tag{4}$$

where Q is the discharge, t is the time, A is the cross-sectional area of the creek, and S_f the frictional slope calculated using a Manning's roughness coefficient $n = 0.025$ as characteristic of open channel flows. Note that in equation (4) is included a term Δ. This term is the momentum loss due to water leaving the creek with its momentum at flood tide to enter the swamp. This momentum is rapidly dissipated in the first few meters of the swamp by friction in the heavily vegetated swamp. At falling tide, the momentum of the water leaving the swamp to flow in the tidal creek is so small that one can safely assume $\Delta = 0$.

The two models, one for the swamp and one for the tidal creek, are linked by the condition that the water levels are the same in the creek and in a swamp cell where they touch each other. The other condition that the outflow from a mangrove cell is the inflow into the tidal creek, and vice-versa, is taken into account through the term q in equations (1) and (3).

Since freshwater runoff is negligible in Coral Creek, the model needs only one open boundary specification, namely a time series of sea level at the mouth.

The model was verified against field observations of currents at two points in the creek: the mouth and a mid-channel point 2 km upstream. Figure 4 shows a comparison between observed and computed tidal currents at the mouth during a spring tide. Note that the peak tidal currents are strong, being greater than 1 m s^{-1}. Also there is a large vertical shear of the currents. Since the waters are vertically well-mixed in salinity and temperature, this shear can be attributed to bottom friction. The model cannot reproduce this vertical shear since it is one-dimensional (vertically averaged). Nevertheless the model appears to be successful in reproducing the main features

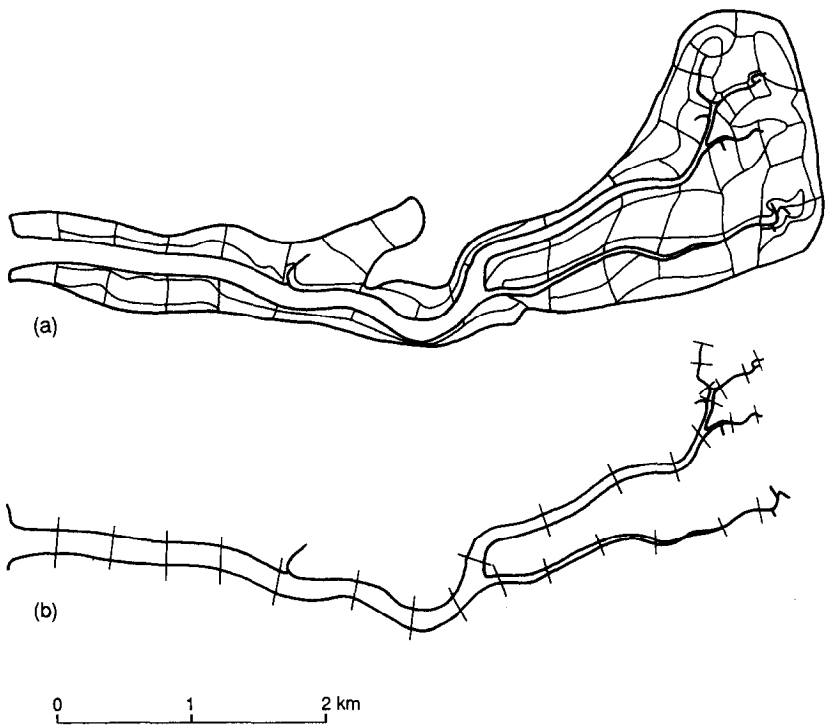

Fig. 3. (*a*) shows the distribution of cells in the mangrove swamp. (*b*) shows the location of the cross-sections.

of the depth-averaged currents, including the tidal asymmetry, the peak ebb tidal currents being much stronger than peak flood currents. The latter peak at 1.2 m s^{-1}, the former at 1.6 m s^{-1}.

This tidal asymmetry results in self-scouring of the tidal creek (Wolanski *et al.*, 1990). Numerical experiments suggest that destruction of the vegetation or reclamation of mangrove land, reduces both the peak tidal currents and the asymmetry of the tidal currents, thereby resulting in siltation of the channel.

Figure 5 shows the distribution of the predicted peak ebb and flood tidal currents in the mangrove swamp. This figures illustrates another important asymmetry of the tidal currents. The flood tidal currents are small, typically of order 0.03 m s^{-1}, and are oriented at about 90° to the banks of the creek. On the other hand, the ebb tidal currents are up to 3 times faster and are oriented at typically 20 to 30° from the creek. This asymmetry in the tidal currents was also confirmed in the field through measurements of currents and current directions at one point in the swamp. Hence, over a tidal cycle there exists in the fringing mangroves a net circulation towards the mouth. The implications of this circulation in the aggregation of mangrove litter are discussed later.

Groundwater flow

In the presence of strong tidal currents such as at Coral Creek, groundwater flow probably does not contribute much to the hydrodynamics of the system. In other cases, groundwater flow may be important. Ovalle *et al.* (1990) have suggested that the net outflow from the small Itacuruca mangrove swamp in Brazil is due to groundwater inflow in the swamp.

Wolanski (unpublished data) and Mazda *et al.* (1990a) have observed the initial stages of the flooding of the swamp at rising tide when a thin sheet of water advances in the swamp from the creek. This sheet is blocked by the high vegetation density. The first few mm of flooding water at a given point are not due to water from that sheet

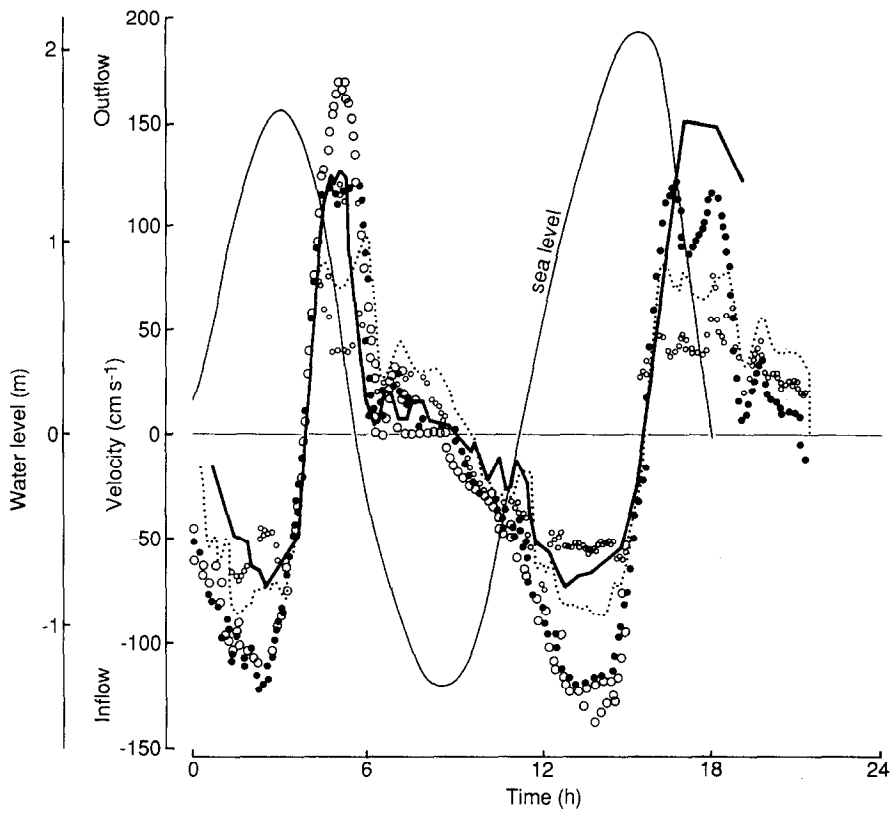

Fig. 4. Time series plot over one tidal cycle of the observed currents at different depths below the surface (from near the surface to near the bottom) at the mouth of Coral Creek; the thick line shows the depth-averaged predicted velocity time series. The thin line is the sea level time series.

spilling over obstructions on the ground, but are observed to come from the ground through the numerous holes due to crabs and rotting vegetation.

Wolanski & Gardiner (1981) have proposed that this groundwater flow is an important flushing mechanism preventing the accumulation of salt left behind after evapotranspiration.

Mazda *et al.* (1990) have carried out a study of groundwater flow in the 200 m long Bashita-Minato mangrove swamp in Japan. After storms, the tidal creek is occasionally ponded by a sill at the mouth. They found that when the creek is ponded the water level in the creek decreases by up to 10 cm day^{-1}, about 15 times larger than the evaporation rate. This observation suggests that the creek was draining out through groundwater flow. The flow appeared to be limited to the upper 90 cm of the substrate, i.e. the maximum depth of crab burrows, since below that point the groundwater was anaerobic.

The importance of crab burrows in enhancing groundwater flow is apparent in Coral Creek and in the Itacuruca swamp, where rainfall infiltrates readily in the soil and produces no local runoff, and in the Klong Ngao mangrove swamp in Thailand where crab burrows are few and direct runoff is observed (Wattayakorn *et al.*, 1990).

Longitudinal diffusion in mangrove creeks

Salinity in mangrove creeks increases with increasing distance from the mouth in the hot dry season when runoff is negligible. The salinity increase is due to evapotranspiration and is typically of order 0.5 to 1 p.p.t. for 5 km long mangrove creeks such as Coral Creek and Dickson

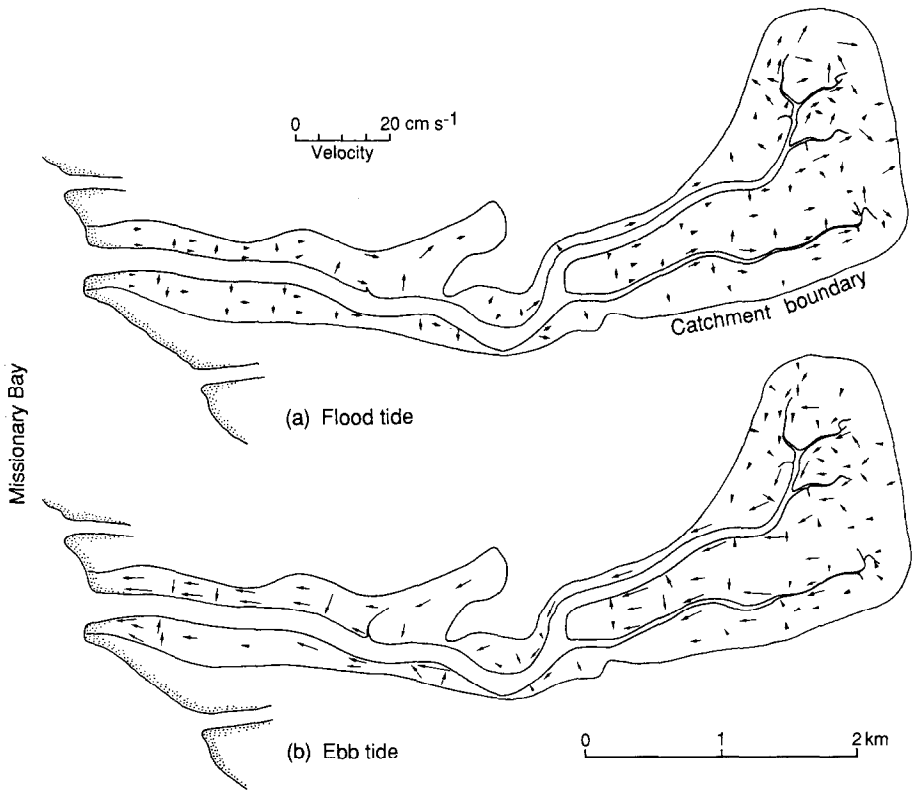

Fig. 5. Predicted peak tidal currents in the mangrove swamp of Coral Creek at flood and ebb tides.

Inlet in Australia (Wolanski *et al.*, 1980; Ridd *et al.*, 1990) and the Klong Ngao mangrove creek in Thailand (Wattayakorn *et al.*, 1990). This salinity gradient can introduce an inverse estuarine circulation as is sketched in Fig. 6a. This circulation becomes hydrodynamically important and measurable when both vertical and horizontal salinity gradients are large. the existence of a vertical gradient is largely dependent on the strength of the tidal currents. In Coral Creek for instance the tidal currents are particularly strong and maintain vertical homogeneity (Fig. 7), except possibly at neap tides. In Dickson Inlet, vertical gradients of salinity are larger, particularly in the upper reaches of the tidal creek (Fig. 8a). The resulting buoyancy effects inhibit vertical turbulent mixing.

In the presence of a small runoff, a salinity maximum zone can develop, which, as sketched in Fig. 6b, essentially isolates the upper reaches of the estuary from the coastal waters. An inverse estuarine circulation exists on either side of the salinity maximum zone. In tropical Australia,

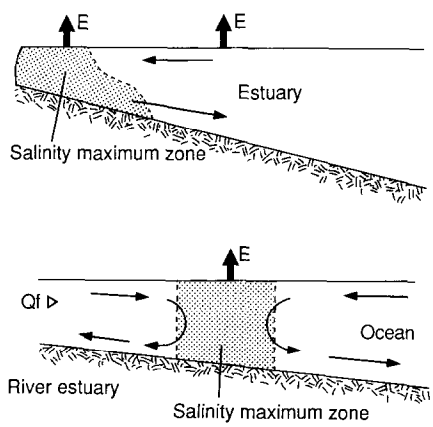

Fig. 6. (*a*) sketches the inverse estuarine circulation generated in a mangrove creek by evapotranspiration in the fringing swamp in the absence of runoff. (*b*) sketches the internal circulation generated by the 'presence of a salinity maximum zone in the presence of a vast evaporation area, such as a vast mangrove swamp, and of a small freshwater runoff.

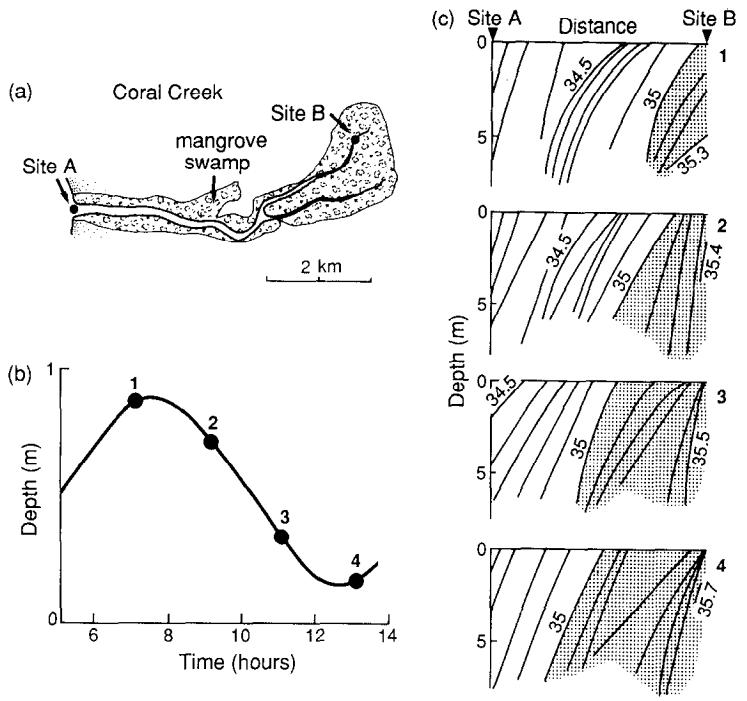

Fig. 7. Longitudinal distribution of salinity in Coral Creek in the hot dry season.

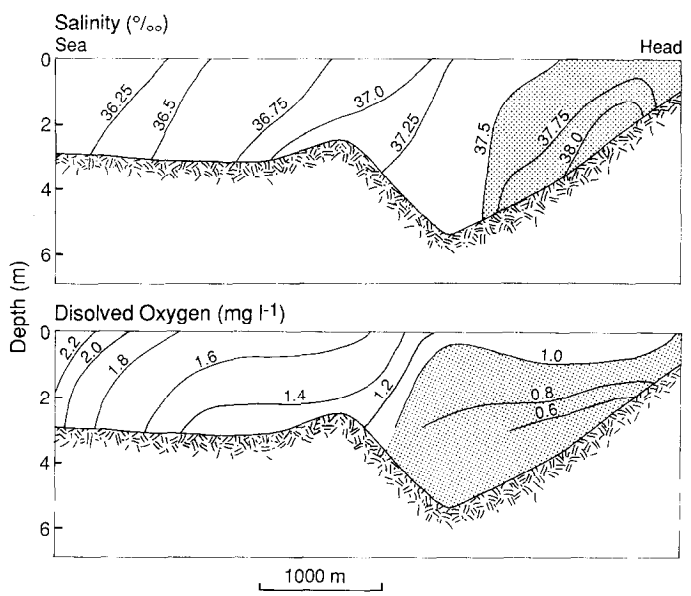

Fig. 8. (*a*) shows the salinity distribution in the Dickson Inlet mangrove creek in the hot dry season, at low tide. (b) shows the corresponding distribution of dissolved oxygen, also at low tide.

such an unusual estuarine circulation can last several months (Wolanski, 1986; Ridd *et al.*, 1988).

In the presence of an inverse estuarine circulation, high salinity mangrove water is then trapped in the creek at the bottom and is not

aerated. The decomposition of the mangrove detritus in that layer and the biological oxygen demand of the mud, can result in low values of the dissolved oxygen concentration (less than 1 mg l^{-1} in Dickson Inlet, Fig. 8b). In some cases anoxic conditions can result, such as occasionally in Coral Creek (Boto, personal communication) and in the Bashito-Minato mangrove swamp (Mazda *et al.*, 1990).

The value of the longitudinal diffusion coefficient, B, hence also the flushing rates, may be estimated from the longitudinal salinity gradient. Since the gradient reaches a steady state, the salt accumulated in the swamp/creek system is exported by tidal diffusion, so that

$$A_t E_t S = BA \frac{dS}{dx} \tag{5}$$

where S is the salinity, E_t the evapotranspiration rate (0.2 to 0.6 cm d^{-1}), A_t the surface area of the swamp, and A is the creek cross-sectional area. Using observed salinity gradients in Coral Creek and the Klong Ngao estuary, equation (5) yields for these two systems

$$B = 20 - 50 \text{ m}^2 \text{ s}^{-1} \tag{6}$$

This value of B is surprisingly large for such small tidal creeks. Indeed, if diffusion was due to vertical turbulent mixing in the creek, then (Bowden & Hamilton, 1975; Fischer *et al.*, 1979) the turbulent eddy diffusivity (B, now called K to differentiate observed from predicted values) would be

$$K = C_d h U \tag{7}$$

where C_d is a drag coefficient, h is the depth and U a characteristic tidal velocity. If vertical motions were dominant, then $Cd = 0.003$. It results $K = 0.03$ m^2 s^{-1} for Coral Creek and the Klong Ngao mangrove creek, a result 1000 times too small. This implies that verticle turbulent motions are not the leading mixing mechanism in mangrove creeks.

Alternatively, following Fisher *et al.* (1979)

$$K = 0.15\, h u_* \tag{8}$$

where u_* is the shear velocity. Nokes (1986) found that

$$u_* = 0.05\, U \tag{9}$$

so that equation (8) becomes

$$K = 0.0075\, hU \tag{10}$$

The value of K from equation (10) is twice that from equation (7). This results in $K = 0.06$ m^2 s^{-1} for Coral Creek and the Klong Ngao mangrove creek, a result still 500 times too small.

Another mixing mechanism may be vertical shear dispersion. This process was first reported by Taylor (1921) for flows in pipes, and has been applied to open-channel flow by Elder (1959) and Fischer *et al.* (1979) who proposed two alternative formulae for diffusion in oscillatory currents,

$$K = 0.1\, Uh$$

or

$$K = 5.93\, hu_* \simeq 0.3\, Uh \tag{11}$$

which for Coral Creek and the Klong Ngao mangrove creek yields $K = 0.5$–1.0 m^2 s^{-1} a value still at least 20 times too small. This suggests that longitudinal diffusion in mangrove-fringed tidal creeks is controlled by another mechanism. This mechanism may be lateral trapping due to lateral shear. Fischer *et al.* (1979) proposed that in a wide, shallow, tidal estuary lateral shear is much more efficient than vertical shear at generating a large longitudinal diffusion. However, their model is not readily applicable to mangrove creeks as it requires a spatially homogeneous lateral shear. More detailed studies of this mechanism are discussed below.

Lateral trapping in mangrove swamps

The previous analytical models of the longitudinal diffusion coefficient in a mangrove creek ne-

glect the presence of the fringing mangrove swamp. In fact this mangrove system is the reason for the existence of a large longitudinal eddy diffusion coefficient in mangrove creeks. The prevailing mechanism is lateral trapping, sketched in Fig. 9. This mechanism was first studied by Okubo (1973) who modeled dispersion in a tidal estuary with a lateral embayment. A tagged water mass moves upstream at flood tide, but a fraction of that mass ends trapped in the embayment. At ebb tide, this mass returns to the tidal creek and mixes with untagged water. Mixing is thus greatly enhanced and, following Okubo (1973),

$$B = \frac{A}{1+\varepsilon} + \frac{\varepsilon u_0^2}{2k(1+\varepsilon)^2(1+\varepsilon+\sigma/k)} \quad (12)$$

where u_0 is the peak tidal current, k^{-1} is the characteristic exchange time between the embayment and the estuary, σ is the tidal frequency and ε is the ratio of volume in the embayment to that in the estuary.

Wolanski & Ridd (1986) modified the Okubo (1973) model to remove two assumptions that are invalid in a mangrove creek, namely that the depths of water in the estuary and in the swamp are the same and are much larger than the tidal range, and that the exchange rate between water in the swamp and in the estuary are constant in time. They divided the mangrove creek in a rectangular main channel where tidal currents occur, and a swamp seen as the lateral embayment. The elevation of the swamp substrate was taken to be higher than mean sea level so that the swamp has

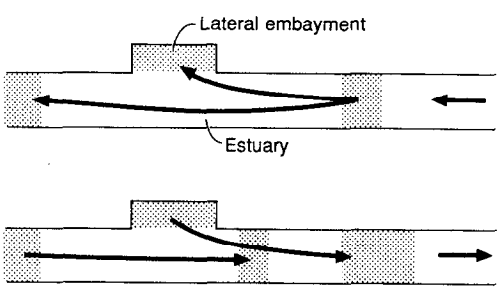

Fig. 9. Sketch of the lateral trapping phenomenon in a tidal estuary with an embayment, adapted from Okubo (1973).

no surface water for a fraction (1-a) of the tidal cycle of period 2T. They predicted

$$B = \frac{A}{(1+\varepsilon)} + \frac{\varepsilon u^2 a^2 T}{48(1+\varepsilon)} \quad (13)$$

Equation (13) yield $B = 10$–$40\ m^2\ s^{-1}$ for Coral Creek, Dickson Inlet and the Klong Ngao estuary, values that agree qualitatively well with observations. Equation (13) was recently modified by Ridd *et al.* (1990) to take into account the decrease in peak tidal velocity from the mouth to the upper reaches of the mangrove creek. Smaller values of the eddy diffusion coefficient are predicted in the upper reaches of the creek particularly in the uppermost 200 m or so.

Lateral trapping in mangrove swamps thus appear to be the dominant effect determining their flushing rate. The residence time in mangrove creeks is of order

$$T_0 = L^2/B \quad (14)$$

where L is the length of the mangrove-fringed creek. For Coral Creek and the Klong Ngao mangrove creek, it results $T_0 = 6$ days, suggesting that the upper reaches of mangrove creeks are flushed slowly.

Wolanski *et al.* (1990) also applied equations (13) and (14) to estimate the values of B and T_0 in Hinchinbrook Channel. They found $T_0 = 50$ days. This implies long-term trapping in this giant mangrove swamp. In fact they found experimental evidence for this long-term trapping in the flushing of brackish water from the channel following cessation of runoff. The salinity deficit followed an exponential decay in time, with an e-fold time scale of 54 days, in surprisingly good agreement with the predictions.

Buoyancy effects in mangrove swamps

Uncles *et al.* (1990) studied the dynamics of a large, mangrove-fringed, estuary in Malaysia. This estuary receives a large fairly steady fresh-

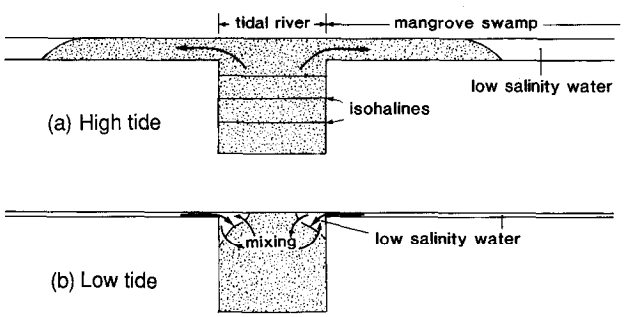

Fig. 10. Cross-channel distribution of salinity in a mangrove-fringed estuary at high and low tide following recovery of the system from a major river flood.

water inflow. They found that the salinity stratification is strong during neap tides but that the system destratifies during spring tides. Water flooding the mangroves is thus fresher at neap tides and saltier at spring tides. This may introduce a cycle, with a period of 2 weeks, in the productivity of the fringing mangrove forest.

Wattayakorn *et al.* (1990) showed that the small mangrove creek of Klong Ngao in Thailand stratifies and destratifies at a few hours period closely following fluctuations in both the tidal currents and in the freshwater inflow which varied rapidly with local short-lived storms in the small, steep watershed draining into that swamp. This unsteadiness precluded a reliable estimate of the outwelling, if any, in the wet season.

In tropical Australia, river runoff can be very intense but short-lived. Salt water can be totally flushed out of the estuary during floods. As soon as the flood is over, salt water creeps back in the estuary. If the estuary is mangrove-fringed, such as the Wenlock River in Australia (Wolanski & Ridd, 1986), the intruding salt water intrudes under the fresh water remaining near the surface. As the tide rises and salt water fills the estuary, the freshwater is pushed back laterally into the fringing mangrove swamps (Fig. 10). This freshwater is then trapped there, with minimal mixing

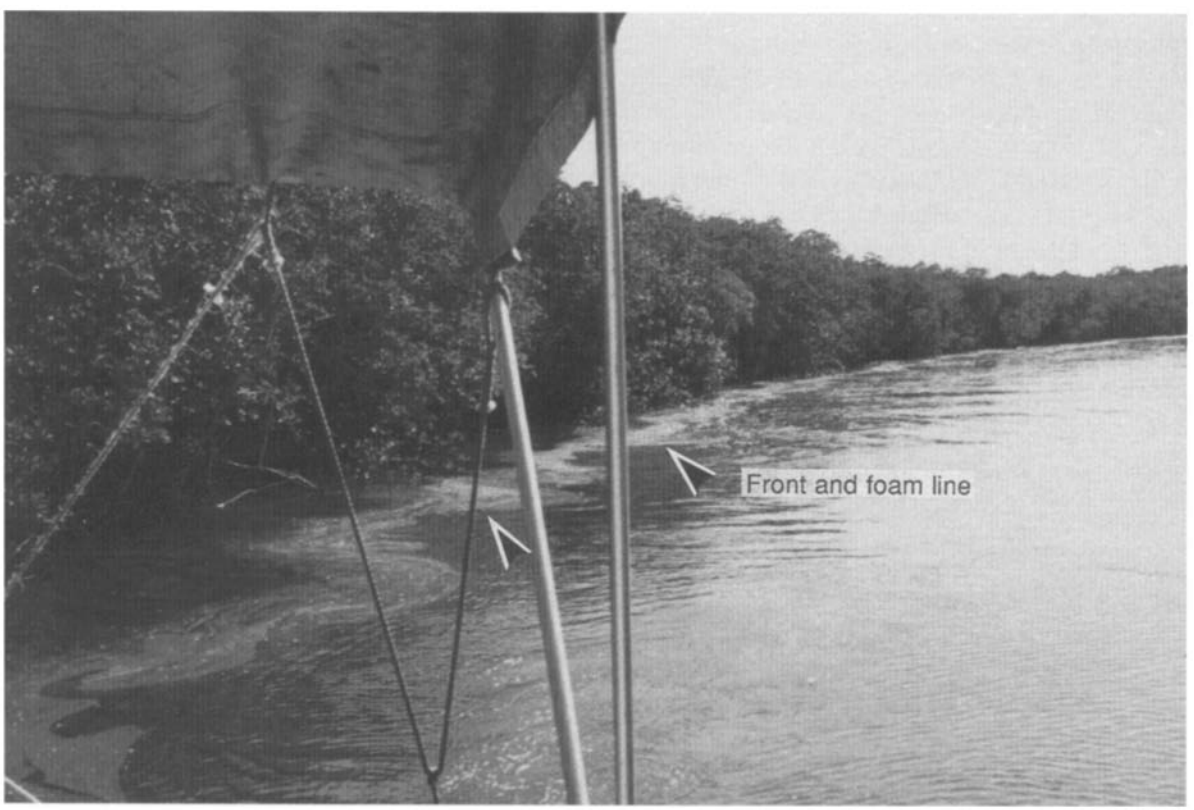

Fig. 11. Photograph showing an oceanographic front separating swamp water from creek waters, and made visible by a foam line.

with salt water in the estuary. As the tide falls, this freshwater returns to the estuary but stays trapped as a narrow river plume in shallow waters along the length of the estuary banks (Fig. 10). In the Wenlock River estuary, this front maintained its integrity throughout the ebb tide. Hence there was minimal mixing between fresh water in the mangrove swamp and sea water in the estuary.

The lateral trapping mechanism prevails also in mangrove creeks and is occasionally made readily visible by the presence of an oceanographic front forming at the start of the ebb tide. This front, shown in Fig. 11, separates swamp water from creek water. In small mangrove creeks, this front disappears in less than an hour but it indicates that the creek is not laterally well-mixed.

The front forming between creek and swamp water is important as it aggregates floating detritus, such as mangrove leaves. Visual observations reveal that at Coral Creek the flood tidal currents are too weak to break the organic film at the surface of the water in the mangrove swamp. Floating mangrove leaves are often trapped in this film and the flood tide does not carry the floating mangrove leaves further inland in the swamp. At ebb tide, the currents are stronger, break the surface film and export floating leaves to the creek. The leaves are then aggregated in long straight lines (foam lines) marking the small-scale oceanographic fronts separating mangrove swamp water from creek water (Fig. 11). These leaves can be outwelled from the mangrove creek to coastal waters where they can sometimes be found, still aligned in a straight line, several km from the swamp in calm weather.

Hence, the fate of mangrove detritus cannot be estimated using classical advection-diffusion models since these models predict that the detritus would be dispersed in a cloud of dimension increasing in time. The formation of small scale barotropic and baroclinic fronts in mangrove swamps has not been studied. These front are important since they result for a depth-averaged model in an apparent negative eddy diffusion as the mangrove seeds and leaves are not dispersed but are instead aggregated. This may have important biological consequences. For instance one often sees small fish aggregating under the leaves

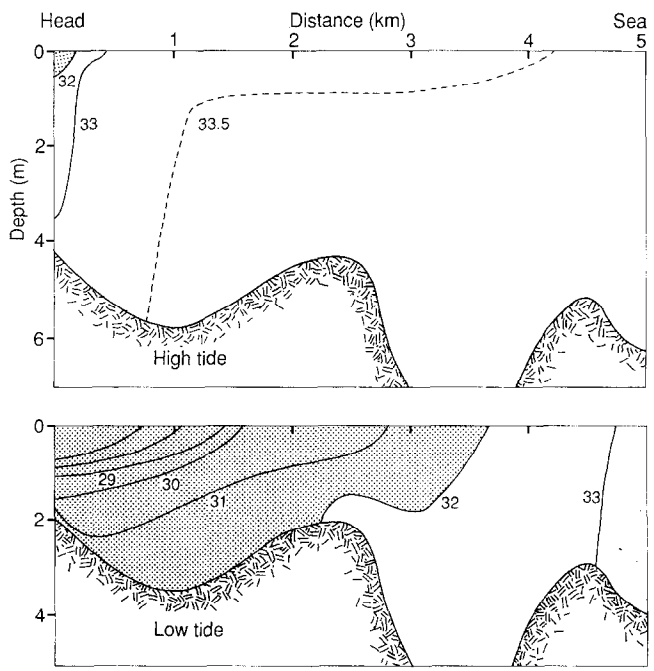

Fig. 12. Longitudinal distribution in Dickson Inlet at high and low tide about 10 days after cessation of runoff.

floating in a small-scale front in a mangrove creek. Wolanski & Hamner (1988) documented several small-scale mechanisms aggregating floating coral eggs. These mechanisms are due to the three-dimensional circulation in topographically controlled fronts. Most of the examples illustrated for reefs can be applied to mangrove creeks. For instance, leaves aggregate downstream of a sharp bend in the mangrove creek even in barotropic conditions as a result of the secondary circulation in a zone of strong flow curvature, in the same manner as coral eggs are aggregated in zones of strong flow curvatures near coral reefs. Axial convergence (Simpson & Turrell, 1986), due to the transverse transport in estuaries, also appears to be a process maintaining the floating leaves and mangrove seeds in a foamline, especially near the mouth of mangrove creeks.

A combination of lateral trapping and buoyancy effects can result in very long residence time of brackish water in mangrove creeks. Figure 12 shows the longitudinal distribution of salinity in mangrove-fringed Dickson Inlet at both low and high tide. Brackish water, a remnant of the runoff 10 days earlier, was still present near the surface in the creek at low tide. At high tide, the bulk of that water was trapped in the swamp. Because buoyancy effects inhibit vertical mixing, the brackish water is basically simply moving back and forth between the swamp at high tide and the creek and low tide, but mixes very little with creek water and is thus only very slowly exported from the system.

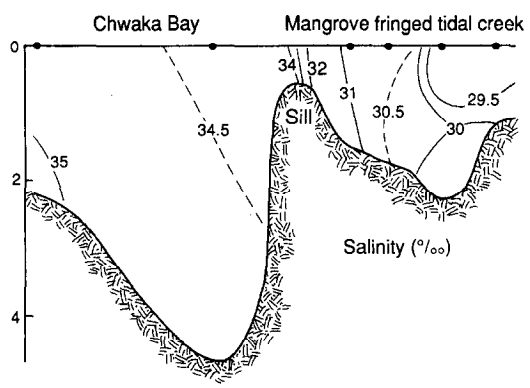

Fig. 13. Longitudinal salinity distribution in the Chwaka bay mangrove swamp in Zanzibar, in the dry season, July 1988.

The presence of a sill or narrow opening increases trapping. For instance, the mangrove creek of Chwaka Bay in Zanzibar is nearly ponded for a measurable portion of the tidal cycle by a small coral limestone sill at the mouth. Strong tidal mixing over shallow water of the sill results in the formation of a front separating creek waters from oceanic waters (Fig. 13). The sill thus inhibits mixing between creek waters and oceanic waters, and ensures long-term trapping in the mangrove-fringed tidal creek (Wolanski, 1989).

Trapping in the coastal zone

Straight coastline

Material outwelled from mangrove swamps may support offshore productivity but, if the coastal waters are shallow, this enrichment is restricted to either a narrow coastal zone or specific points near headlands.

When runoff is important, the outwelled material remains in the river plumes. In areas where river runoff is always important, such as on the mangrove-fringed coast of Thailand facing the Andaman Sea near Burma, longshore currents ensure that these river plumes usually remain coastally trapped together with the outwelled mangrove detritus and nutrients (e.g. Wattayakorn *et al.*, 1990). Any nutrient enrichment from the mangrove is then limited to coastal waters. Similar coastal trapping of steady river plumes for hundreds of km has been reported in Nicaragua (Murray & Young, 1985) and in South America (Bouyne & Roux, 1978).

In tropical Australia, river runoff is short-lived. Freshwater is injected into coastal waters in a pulse-like event. Once runoff ceases, tidal currents maintain vertical homogeneity in shallow coastal waters, and the brackish waters behave more or less like a passive tracer. The fate of this tracer, i.e. the time it takes to be flushed out from coastal waters, provides a good indication of the dynamics of the coastal zone. Two examples are illustrated below: the Gulf of Carpentaria and the coast of the Great Barrier Reef.

Figure 14 shows the distribution of salinity in the Gulf of Carpentaria at 3 monthly interval in 1976. The survey in April–May corresponds to the end of the wet season. It shows that the brackish water was coastally trapped and did not mix readily with offshore waters. Five months after, in August–September, runoff was negligible but brackish water was still found in the shallow coastal waters (depth less than 15 m or so). This finding suggests that brackish waters is trapped for several months in a coastal boundary layer, and that cross-shelf mixing between offshore waters and coastal boundary layer water is very slow (Wolanski & Ridd, 1990). A satellite image in the visible bands taken in calm weather (no wind stirring of bottom sediment) in the very dry season of November, 1986 (zero runoff hence no river plume) also shows a band of water of different colour in the dry season (negligible runoff) along the coast of the Gulf of Carpentaria, with a front running along the 15–20 m isobath (Fig. 15). The presence of a coastal boundary layer may be explained by the effects of friction in shallow water. Figure 16 shows the predicted mean Eulerian circulation under the action of both the tides and wind in the tradewind season. This shows a narrow coastal jet extending to the 15 to 20 m isobath with a return flow in deeper water. The tides alone drive a negligible net circulation even in shallow coastal waters, while wind alone in the absence of tides drives a coastal jet about 3 times as wide as that shown in Fig. 16 (Wolanski & Ridd, 1990). The non-linear interaction between tidal currents and wind-driven currents is an essential factor in the dynamics of the coastal boundary layer.

Rugged coastline

The east coast of the Gulf of Carpentaria is fairly straight, with no major headlands, and extensive areas of shallow waters, the 20 m isobath being located 20 km offshore. In contrast, the Great Barrier Reef continental shelf has numerous headlands (Fig. 17) and the waters are deeper, the 20 m contour line nearly touching these headlands. The salinity distribution in coastal waters was measured after the flooding of the Burdekin River and other smaller streams in January 1981. This distribution is shown in Fig. 17 for 26–27 January 1981, about 3 days past the peak of the flood and for 3–4 February 1981, 10 days after the flood. Note that in the first survey the plume moved northward but was continuous over 200 km and coastally trapped with the coast on its left-hand-side, as dictated by Coriolis forces, though offshore the current was southward (Wolanski & van Senden, 1983). In the second survey, the plume was broken up in patches. Brackish water remained preferentially in the wide bays sheltered by headlands.

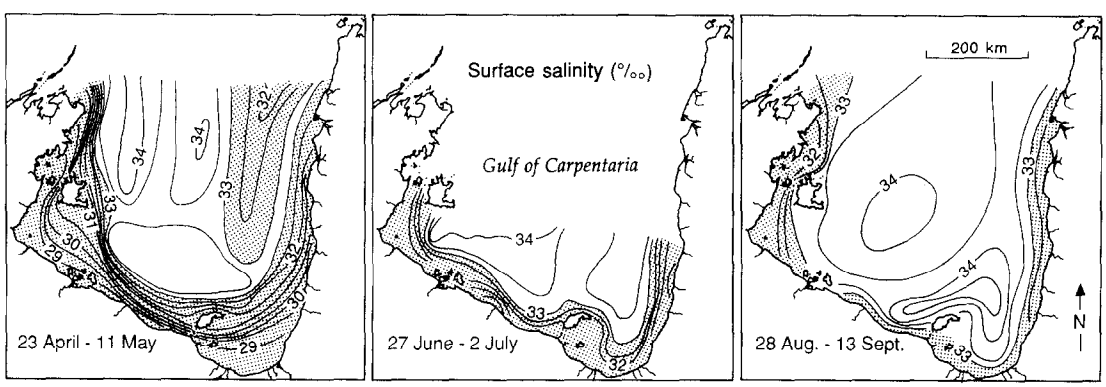

Fig. 14. Salinity distribution in the Gulf of Carpentaria at about three-monthly interval in 1976. These data were kindly provided by P. Rothlisberg.

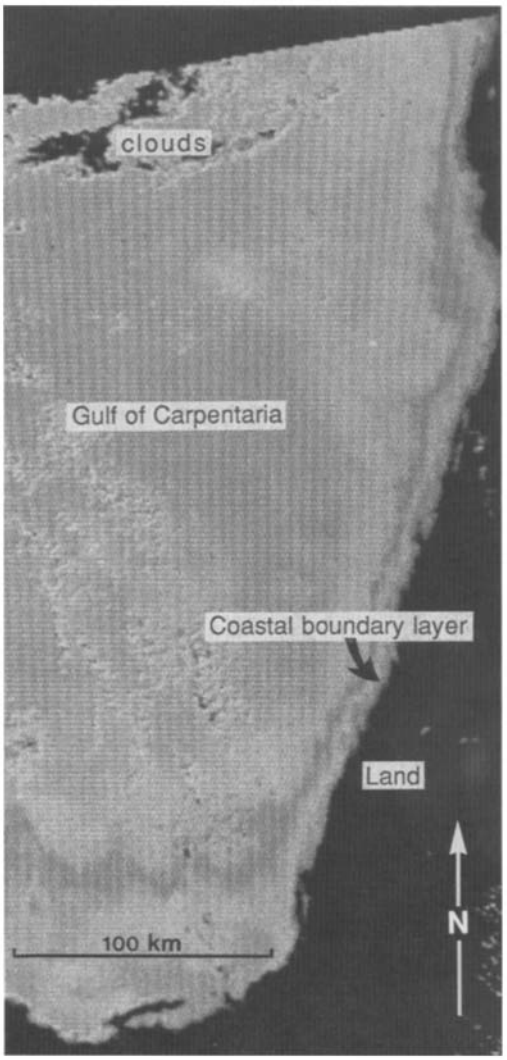

Fig. 15. NOAA satellite view in the visible bands of the east and south coasts of the Gulf of Carpentaria on 23 November 1986, during the hot dry season, in calm weather.

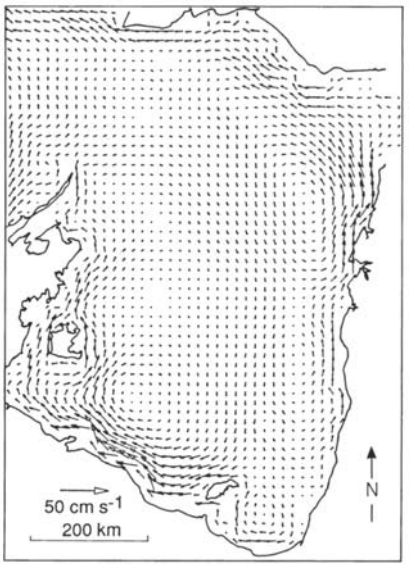

Fig. 16. Predicted mean circulation in the Gulf of Carpentaria under the combined influence of all tides and a 15 m s^{-1} southeasterly trade-wind.

Mixing and dispersion near headlands

These data imply that coastal trapping is much less efficient on the Great Barrier Reef coast than in the Gulf of Carpentaria. This difference may be attributed to the headlands and reefs on the Great Barrier Reef continental shelf, these obstructions to flow being absent in the Gulf of Carpentaria. Flow around headlands and islands generate eddies (Pingree & Maddock, 1979; Wolanski *et al.*, 1984; Falconer *et al.*, 1986; Pattiaratchi *et al.*, 1987; Geyer & Signell, 1990). The two most intensive field studies of currents around a headland or an island in shallow waters have been those of Wolanski *et al.* (1984) and Geyer & Signell (1990). Wolanski *et al.* (1984) documented the presence of energetic island wakes from the data from 24 current meters, float measurements, CTD studies and aerial photography. Geyer & Signell (1989) measured the circulation around a headland using a ship-mounted acoustic Doppler current profiler. Figure 18 shows an example of a fully developed, energetic headland eddy as measured with this latter technique.

Wolanski *et al.* (1984) and Falconer *et al.* (1986) have proposed respectively analytical and numerical models that attempt to explain these eddies in terms of vorticity dynamics at respectively steady and unsteady cases. Their models rely strongly on flow separation dynamics at the separation points at the island's tips. Black & Gay (1977) criticised the vorticity model and claimed that the eddy strength was not primarily governed by flow separation, but is a 'phase eddy' formed as a result of the oscillatory pressure gradient, which near the end of the half cycle, reverses the frictionally controlled flow near the

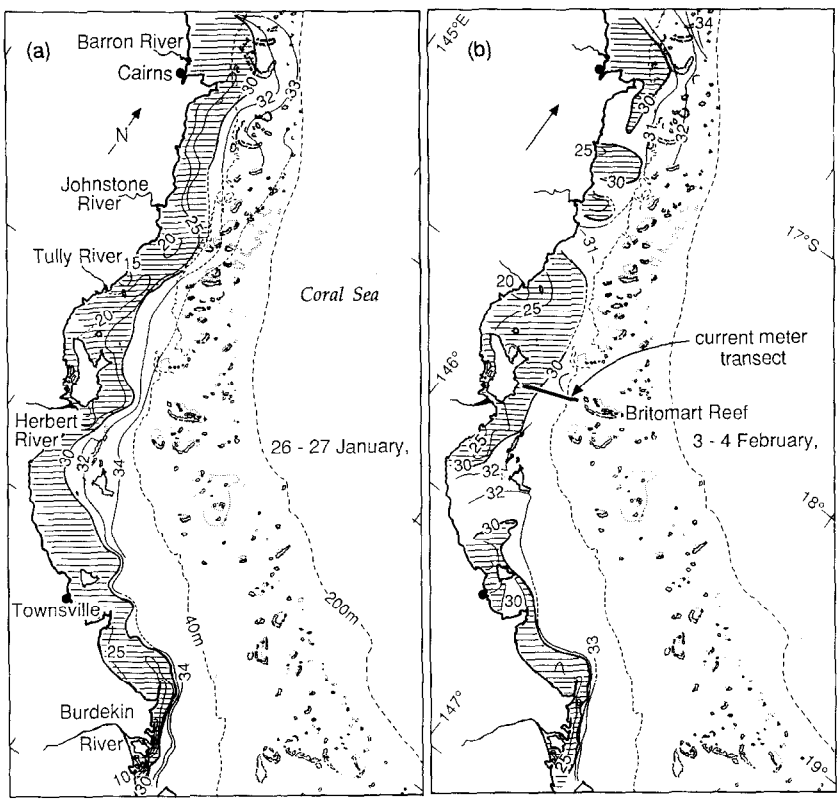

Fig. 17. Surface salinity distribution on the Great Barrier Reef continental shelf between the mouth of the Burdekin River and Cairns, following flooding of the Burdekin River and other smaller streams, in 1981.

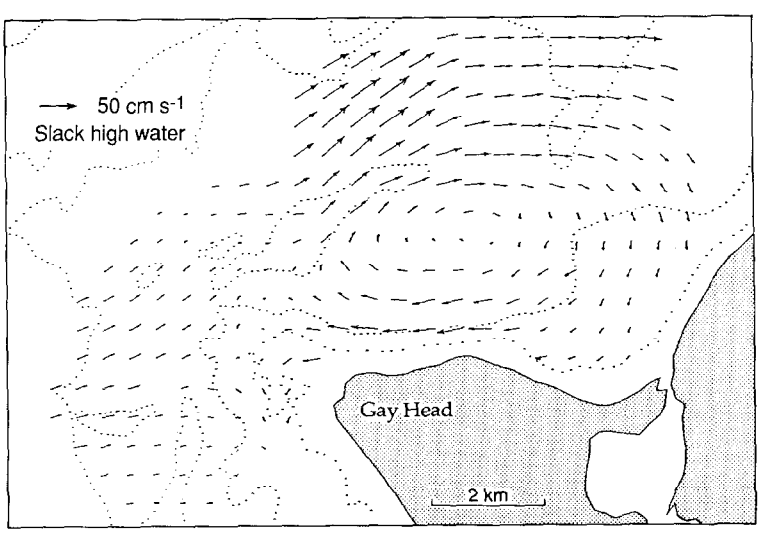

Fig. 18. Observations of the velocity field and evidence for a strong eddy behind Gay Head, Massachusetts, USA, adapted from Geyer & Signell (1990).

coast before the freestream flow. However, Signell (1989) carried out the most detailed, small-scale, numerical studies so far of headland wakes, and showed that the vorticity which forms transient eddies is produced near the headland tip and that flow separation is indeed critical to transport this vorticity into the interior of the eddy.

Deleersnijder *et al.* (1989) have developed a three-dimensional model of the tidal wakes and showed that, though the eddy dynamics are essentially two-dimensional (independent of depth), there exist nevertheless vertical motions, with upwelling near the center of the eddy and downwelling along the island sloping boundaries, as shown in Fig. 19.

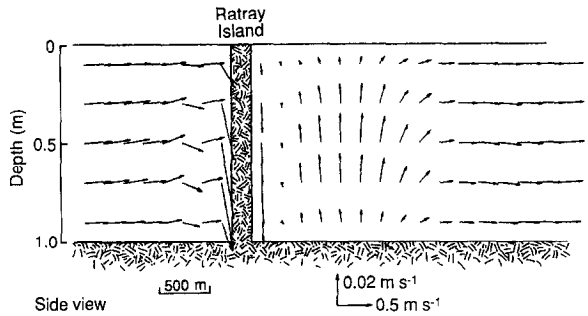

Fig. 19. Numerical predicted three-dimensional circulation around Rattray Island, Australia, after eddy spin-up. This figure shows the velocity field in a vertical plane oriented along the mean flow direction and intersecting the middle of the island. Adapted from Deleersnijder *et al.* (1989).

Signell (1989) also showed the importance of adequate grid resolution near the headland tip. He showed that a lack of small-scale resolution in that area leads to an underestimate of the wake strength (Tee, 1976). This is not simply of academic interest, but has profound implications for modeling the fate of water-borne material. The inclusion, or the neglect, of flow separation effects in numerical models lead to quite different results. When flow separation is included, patches of contaminants in the vicinity of the headlands are strongly deformed by straining associated with the separated shear layer and transient vortices (Signell, 1989). As is shown in Fig. 20, the distribution of material is extremely patchy and streaky for those contaminants entrained in the free shear layers, while those contaminants not entrained in the free shear layers are essentially carried through with minimal mixing. Figure 20 demonstrates that the large strain rate in the region of flow separation tends to stretch particles of fluid into long filaments, which are subsequently rolled and distorted by the transient eddy field (Geyer & Signell, 1990; Signell & Geyer, 1990).

The intense shear associated with the flow separation at the tip of the headland, is the agent responsible for the nearly explosive dispersion of the patch that started close to the headland in Fig. 20. Evidence for such patchiness and streakiness is found in field experiments of dispersion around coral reefs (e.g. Wolanski & Hamner, 1988; Wolanski *et al.*, 1988; Wolanski & King, 1990). On the other hand, models that neglect

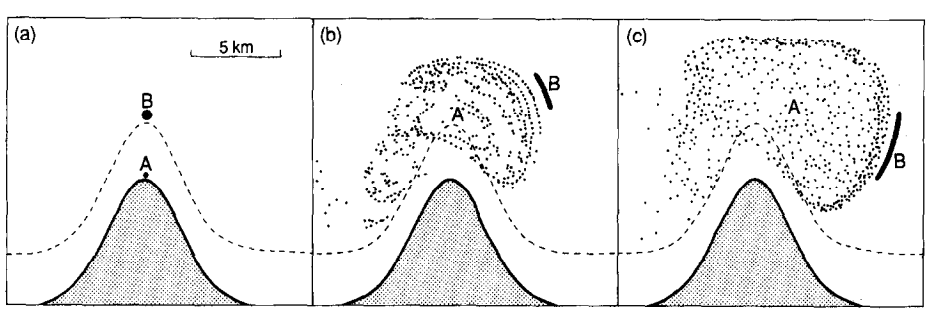

Fig. 20. Numerically predicted dispersion around a headland with reversing tidal currents in the absence of any net currents. Two patches of particles are released at the beginning of the eastward flowing tide, one just off the tip of the headland and the other some distance offshore (*a*). (*b*) shows the distribution after 6 tidal cycles, and (*c*) after 12 tidal cycles. Adapted from Signell & Geyer (1990).

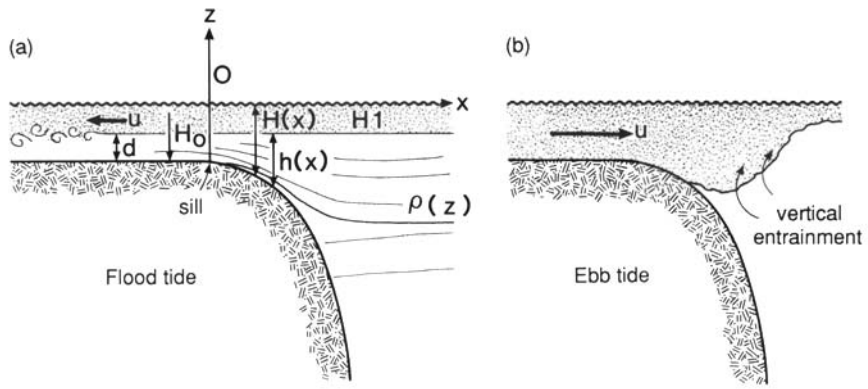

Fig. 21. Upwelling in a tidal jet at (*a*) flood tide and (*b*) ebb tide.

these flow separation dynamics, such as the 'phase eddy' model, are unreliable because they result in smooth distributions from gradient-type diffusion since they do not simulate straining and folding of vortex lines.

The inclusion, or no inclusion, of separation flow effects in numerical models, is not just a question of academic interest only. Indeed, the numerical models used at present to simulate the dispersal of crown-of-thorn starfish in the Great

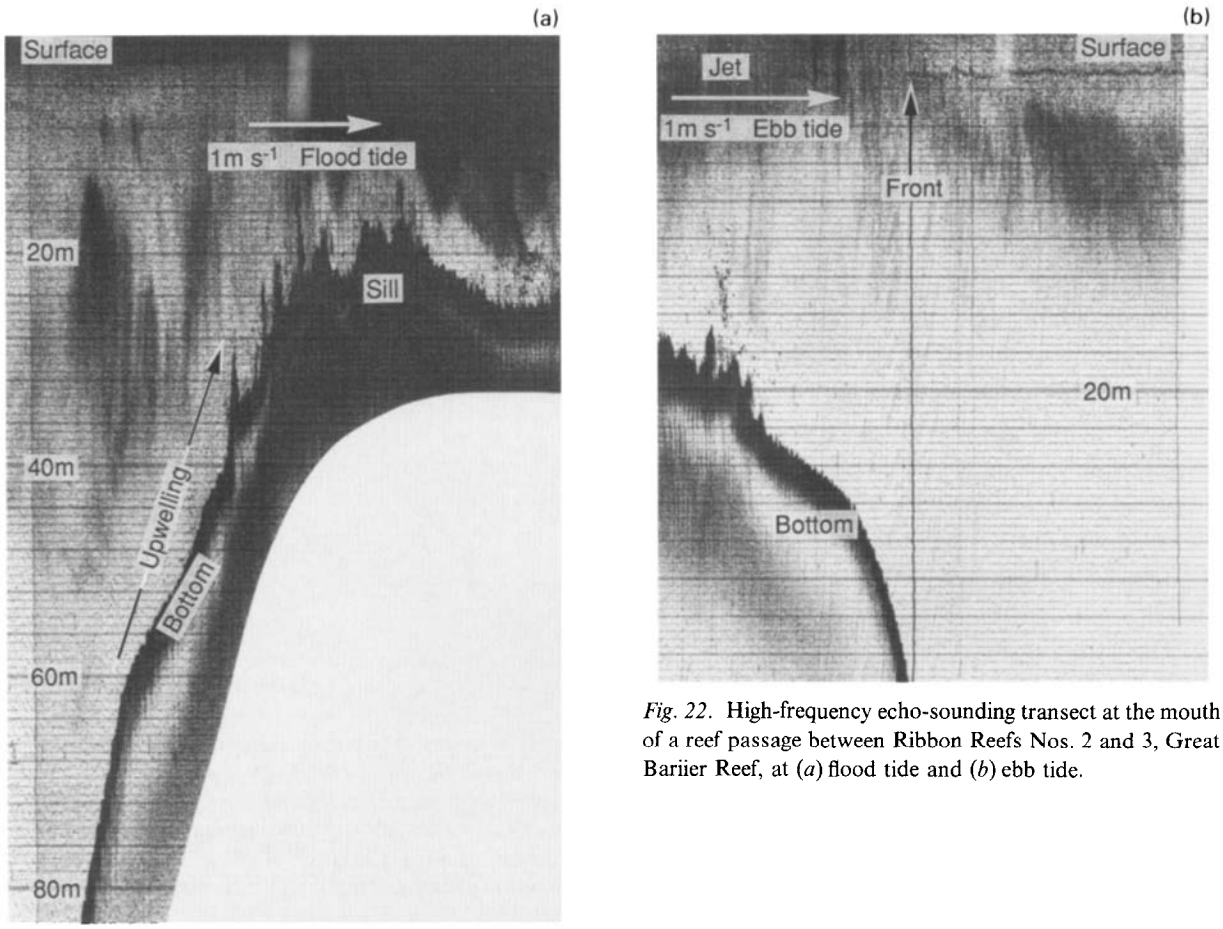

Fig. 22. High-frequency echo-sounding transect at the mouth of a reef passage between Ribbon Reefs Nos. 2 and 3, Great Bariier Reef, at (*a*) flood tide and (*b*) ebb tide.

Barrier Reef, a problem of great practical and management importance, neglect these dynamics and predict smooth distributions and long retention times near reefs (e.g. Black, 1988). Such model predictions are contrary to expectations if straining and folding of vortex lines were included in the models.

Another important mixing mechanism is that of tidal jet-vortex pair system, the dynamics of which is also intimately linked with flow separation effects (Awaji *et al.*, 1980; Awaji, 1982; van Senden, 1985; Wolanski *et al.*, 1988). Awaji *et al.* (1980) and Awaji (1982) found that the pattern of transport and dispersion varies greatly over short length scales and, exactly as in the case of island wakes, does not display the smearing tendency of a typical diffusive process.

Usually mangrove-fringed coastal waters are sufficiently shallow that, through friction (Ozsoy, 1977), tidal jets do not prevail at ebb tides at the mouth of tidal creeks (Wolanski & Ridd, 1990). The frictional slope term balances the surface slope term in the continuity equation, and thus the flow resembles potential flow. However, there exist some mangrove creeks, e.g. Tudor Creek in Mombasa, Kenya, that face deep water. Complex and biologically important flow patterns probably exist at such places and may resemble that observed in front of reef passages through the Ribbon Reefs, Great Barrier Reef of Australia (Thompson & Golding, 1981; Wolanski *et al.*, 1988). At flood tide, forced upwelling may occur as a result of the strong tidal currents at the mouth, as is sketched in Fig. 21a. This upwelling is readily visible in high-frequency echo-soundings, the scatterer probably being plankton (Fig. 22a). At ebb tide, a tidal jet may also develop, lifting off the bottom as a result of buoyancy effects, and resulting in upwards entrainment of deep water in the jet (Fig. 21b). High-frequency echo-soundings (Fig. 22b) also confirm the existence of such a mechanism.

Though a rugged coastline prevents the formation of a long, stable coastal boundary layer, trapping can occur in the shallow embayments sheltered by headlands such as Bowling Green bay, a wide, shallow embayment near Townsville, Australia (Fig. 23). The primary reason for this is that, because of friction, neither headland eddies nor the longshore currents found further offshore are generally able to propagate in these very shallow, sheltered, waters (Wolanski & Ridd, 1990).

Trapping is reinforced when the embayments are mangrove-fringed. Such is the case for instance at the northern region of Hinchinbrook Channel where the west coast is mangrove-fringed and very shallow (Fig. 24a). Water moves back and forth with the tides between the mangrove swamp and the coastal boundary layer in shallow

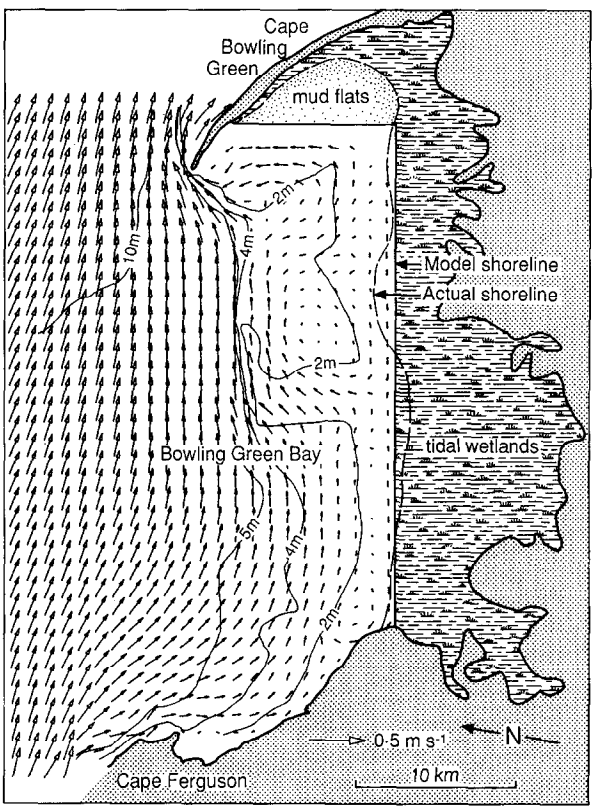

Fig. 23. Net circulation in Bowling Green Bay, a shallow mangrove-fringed embayment near Townsville, Australia, in calm weather. Tides and the southward flowing East Australian Current generate strong currents offshore. The bathymetry is in metres. The bay has extensive tidal wetlands. To make the very small nearshore currents visible on this graph together with the strong offshore currents, the length of the velocity arrows is proportional to the logarithm of the water currents. As a result a factor of 10 difference in the water velocity implies a difference by a factor of 2 in the length of the arrows.

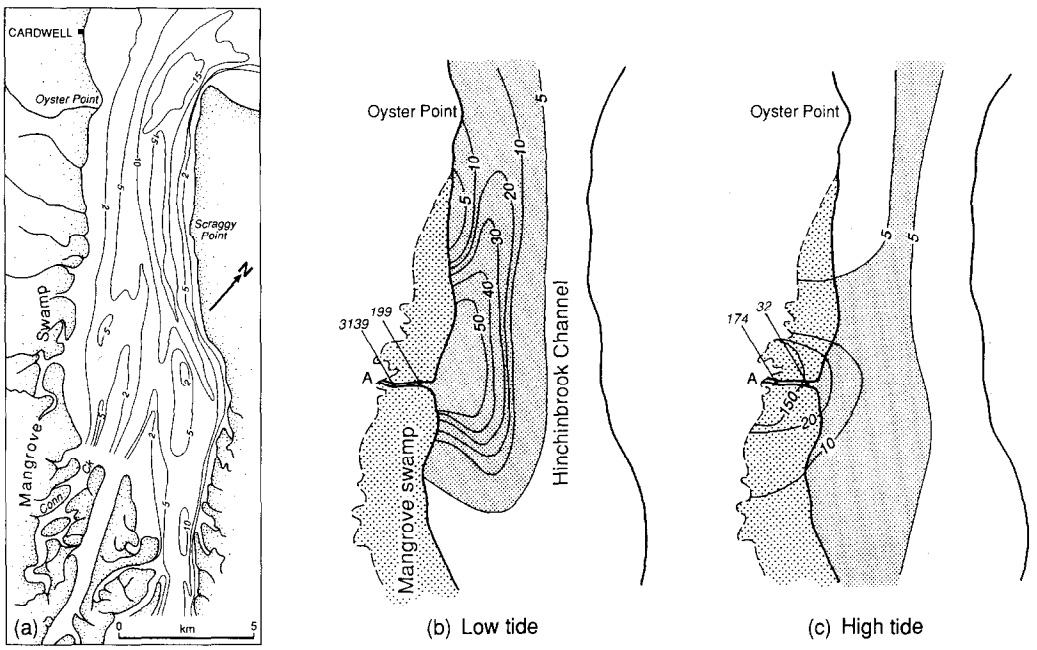

Fig. 24. (*a*) Map of the northern region of Hinchinbrook Channel with depths in m. (*b*) and (*c*) show the plume, at low and high tide, of a tracer after 15 days of continuous discharge at point A in the upper reaches of a mangrove creek in calm weather.

waters on the west coast. The coastal boundary layer waters being very shallow, there is little cross-shelf mixing between coastal boundary layer waters and waters further offshore in the deeper parts of the channel. Wolanski *et al.* (1990) have modeled the water circulation in this area. The mangrove swamps were considered to be inter-tidal storage areas. The model results were verified against field observations of currents. A tracer was released continuously for 15 days at point A in the model, in the upper reaches of a mangrove creek, and followed through time. Figure 24 (b and c) shows the tracer's plume at both low tide and high tide after 15 days in calm weather. The contaminant is found in shallow coastal waters at low tide, and the bulk of this contaminant is found trapped in the mangrove swamp at high tide.

The presence of a coastal boundary layer in shallow, mangrove-fringed, coastal waters, presents problems in interpreting outwelling studies based on a budget of material exported over a tidal cycle by a mangrove creek (e.g. Boto & Bunt, 1981) since water entering a mangrove creek in such areas may simply have left another nearby creek at the previous tidal cycle and is chemically different from offshore water. Thus a mangrove creek at the upstream side of a coastal boundary layer will have an apparent lower bulk return coefficient than one at the downstream end.

Under the action of wind and tides, coastal boundary layer waters, enriched in nutrient by outwelling from the tidal wetlands, can be ejected offshore as tidal jets peeling off capes and headlands (Bowman, 1988; Wolanski & Ridd, 1990). This process may explain the presence of baitfish and billfish schools found a few km offshore from Cape Bowling Green (Williams, 1988).

References

Awaji, T. A., N. Imasato & H. Kunishi, 1980. Tidal exchange through a strait: A numerical experiment using a simple model basin. J. Phys. Oceanogr. 10: 1499–1508.

Awaji, T., 1982. Water mixing in a tidal current and the effect ot turbulence on tidal exchange through a strait. J. Phys. Oceanogr. 12: 501–514.

Black, K. P., 1988. The relationship of reef hydrodynamics to variation in number of planktonic larvae on and around

coral reefs. Proc. 6th. Int. Coral Reef Symposium, Townsville, Vol. 2.

Black, K. P. & S. L. Gay, 1987. Eddy formation in unsteady flows. J. geophys. Res. 92: 9514–9522.

Boto, K. & J. S. Bunt, 1981. Tidal export of particulate organic matter from a northern Australian mangrove system. Estuar. coast. Shelf Sci. 13: 247–255.

Bowden, K. F. & P. Hamilton, 1975. Some experiments with a numerical model of circulation and mixing in a tidal estuary. Estuar. coast. Mar. Sci. 3: 281–301.

Bowman, M. J., 1988. Estuarine fronts. In B. Kjerfve (ed.), Hydrodynamics of estuaries, Vol. 1, CRC Press, Boca Raton, Florida, 85–132.

Bouyne, P. & J. D. Roux, 1978. Remarques sur la circulation d'eaux turbides d'origine amazonienne le long de la cote des Guyanes. C.r. Acad. Sci. Paris, 287, Serie D.: 203–205.

Burke, R. W. & K. H. Stolzenbach, 1983. Free surface flow through salt marsh grass. Massachusetts Institute of Technology Sea Grant College Program, Publication No. MITSG 83-16, Cambridge, MA., 252 pp.

Deleersnijder, E., E. Wolanski & A. Norro, 1989. Numerical simulation of the three-dimensional tidal circulation in an island's wake. In G. M. Carlomagno & C. A. Brebbia (eds), Computer and experiments in fluid flow. Computational Publications, Springer-Verlag, Berlin: 355–381.

Elder, J. W., 1959. The dispersion of marked fluid in turbulent shear flow. J. Fluid Mech. 5: 544–560.

Falconer, R. A., E. Wolanski & L. Mardapitta-Hadjipandeli, 1986. Modelling tidal circulation in an island's wake. J. Waterway, Port, Coastal and Ocean Engineering, ASCE, 112: 234–254.

Fischer, H. B., E. J. List, R. C. Y. Koh, J. Imberger & N. H. Brooks, 1979. Mixing in inland and coastal waters. Academic Press, New York, 484 pp.

Geyer, W. R. & R. P. Signell, 1990. A reassessment of the role of tidal dispersion in estuaries and bays. Estuaries, in press.

Geyer, W. R. & R. P. Signell, 1990. Measurements of tidal flow around a headland with a shipboard acoustic Doppler current profiler. J. geophys. Res. 95: 3159–3197.

Mazda, Y., Y. Sato, S. Swamoto, H. Yokochi & E. Wolanski, 1990. Links between physical, chemical and biological processes in Bashita-Minato, a mangrove swamp in Japan. Estuar. coast. Shelf Sci., in press.

Mazda, Y., H. Yokochi & Y. Sato, 1990. The behaviour of groundwater in a mangrove area and the influence on the properties of water and bottom mud. Estuar. coast. Shelf Sci. 31: 621–638.

Murray, S. P. & M. Young, 1985. The nearshore current along a high-rainfall, tradewind coast – Nicaragua. Estuar. Coast. Shelf Sci. 21: 687–699.

Nokes, R. I., 1986. Problems in turbulent dispersion. Ph.D. Thesis, Dept. Civil Eng., Univ. of Canterbury, Christchurch, New Zealand, 229 pp.

Okubo, A., 1973. Effect of shoreline irregularities on streamwise dispersion in estuaries and other embayments. Neth. J. Sea Res. 6: 213–224.

Ovalle, A. R. C., C. E. Rezende, L. D. Lacerda & C. A. R. Silva, 1990. Factors affecting the hydrochemistry of a mangrove tidal creek, Sepetiba Bay, Brazil. Estuar. coast. Shelf Sci.: 639–650.

Ozsoy, E., 1977. Flow and mass transport in the vicinity of tidal inlets. Technical Rep. UFL/COEL/TR-036, Coastal and Oceanographic Engineering Department, University of Florida.

Pattiaratchi, C., A. James & M. Collins, 1987. Island wakes and headland eddies: a comparison between remotely sensed data and laboratory experiments. J. geophys. Res. 92: 783–794.

Petryk, S. & G. Bosmajan, 1975. An analysis a flow through vegetation. J. Hydraul. Div., Am. Soc. Civil Eng. 101: 871–874.

Pingree, R. D. & L. Maddock, 1979. The tidal physics of headland flows and offshore tidal bank formation. Mar. Geol. 32: 269–289.

Ridd, P. V., M. W. Sandstrom & E. Wolanski, 1988. Outwelling from tropical tidal salt flats. Estuar. coast. Shelf Sci. 26: 243–253.

Ridd, P. V., E. Wolanski & Y. Mazda, 1990. Longitudinal diffusion in mangrove-fringed tidal creeks. Estuar. coast. Shelf Sci. 31: 541–554.

Robertson, A. I., D. M. Alongi, P. Daniel & K. G. Boto, 1988. How much mangrove detritus enters the Great Barrier reef lagoon? Proc. 6th. Inter. Symp. Coral Reefs, Townsville, Aug. 1988.

Signell, R. P., 1989. Tidal dynamics and dispersion around coastal headlands. Ph.D. thesis, MIT/WHOI-89-38.

Signell, R. P. & W. R. Geyer, 1990. Numerical simulation of tidal dispersion around a coastal headland. In R. T. Cheng (ed.), Residual currents and long-term transport in estuaries and bays, Lecture notes on Coastal and Estuarine Studies, Springer-Verlag: 210–222.

Simpson, J. H. & I. D. James, 1986. Convergent fronts in the circulation on tidal estuaries. In D. A. Wolfe (ed.), Estuarine variability. Academic Press, London.

Taylor, G. I., 1921. Diffusion by continuous movements. Proc. London Math. Soc., Ser. A, 20: 196–211.

Tee, K. T., 1976. Tide-induced residual current, a 2-D nonlinear numerical tidal model. J. Mar. Res. 34: 603–628.

Thompson, R. O. R. Y. & T. J. Golding, 1981. Tidally induced upwelling by the Great Barrier Reef. J. geophys. Res. 86: 6517–6521.

Uncles, R., J. E. Ong & W. K. Gong, 1990. Observations and analysis of a stratification-destratification event in a tropical estuary. Estuar. coast. Shelf Sci. 31: 651–666.

van Senden, D., 1985. Structure of tidal jets under variable source conditions. Proc. 21st Congress I.A.H.R., Melbourne, 3C, pp. AI/3–AI/8.

Wattayakorn, G., E. Wolanski & B. Kjerfve, 1990. Mixing, trapping and outwelling in the Klong Ngao mangrove swamp, Thailand. Estuar. coast. Shelf Sci., in press.

Williams, D. McB., 1988. Significance of coastal resources to sailfish and blackmarlin in NE Australia: an on-going re-

search program. Proc. International Billfish Symposium II, Kailua-Kona, Hawaii, Aug. 1–5, 1988.

Wolanski, E., 1986. An evaporation-driven salinity maximum zone in Australian tropical estuaries. Estuar. coast. Shelf Sci. 22: 415–424.

Wolanski, E., 1989. Measurements and modeling of the water circulation in mangrove swamps. UNESCO-COMARAF Serie Documentaire No. 3, 43 pp.

Wolanski, E., 1989. Circulation anomalies in tropical Australian estuaries. In B. J. Kjerfve (ed.), Hydrodynamics of estuaries. Vol. II, CRC Press, Boca Raton: 53–59.

Wolanski, E. & R. Gardiner, 1981. Flushing of salt from mangroves. Aust. J. mar. Freshwat. Res. 32: 681–683.

Wolanski, E. & W. M. Hamner, 1988. Topographically controlled fronts in the ocean and their biological influence. Science 241: 177–181.

Wolanski, E. & B. King, 1990. Flushing of Bowden Reef lagoon. Estuar. coast. Shelf Sci. 31: 789–804.

Wolanski, E. & P. Ridd, 1986. Tidal mixing and trapping in mangrove swamps. Estuar. coast. Shelf Sci. 23: 759–771.

Wolanski, E. & P. Ridd, 1990. Mixing and trapping in Australian tropical coastal waters. In R. T. Cheng (ed.), Residual currents and long-term transport in estuaries and bays. Lecture notes on Coastal and Estuarine Studies, Springer-Verlag: 165–183.

Wolanski, E. & D. van Senden, 1983. Mixing of Burdekin River flood waters in the Great Barrier Reef. Austr. J. mar. Freshwat. Res. 34: 49–63.

Wolanski, E., D. Burrage & B. King, 1989. Trapping and dispersion of coral eggs around Bowden Reef, Great Barrier Reef, following mass coral spawning. Contin. Shelf Res. 9: 479–496.

Wolanski, E., J. Imberger & M. L. Heron, 1984. Island wakes in shallow coastal waters. J. geophys. Res. 89: 10553–10569.

Wolanski, E., M. Jones & J. S. Bunt, 1980. Hydrodynamics of a tidal creek-mangrove swamp system. Aust. J. mar. Freshwat. Res. 31: 431–450.

Wolanski, E., E. Drew, K. Abel & J. O'Brien, 1988. Tidal jets, nutrient upwelling, and their influence on the productivity of the alga Halimeda in the Ribbon Reefs, Great Barrier Reef. Estuar. coast. Shelf Sci. 26: 169–201.

Wolanski, E., Y. Mazda, B. King & S. Gay, 1990. Dynamics, flushing and trapping in Hinchinbrook Channel, a giant mangrove swamp, Australia. Estuar. coast. Shelf Sci. 31: 555–580.